

Certainly, there is much work to be done, but now that it is known to be feasible to analyze these complex systems with the help of computers, we need not hesitate to undertake the necessary experiments.

#### ACKNOWLEDGMENTS

We are indebted to Dr. R. M. Diamond, Professor I. Halpern, and Professor H. Morinaga for helpful discussions.

PHYSICAL REVIEW

VOLUME 157, NUMBER 4

20 MAY 1967

## Emission of Alpha Particles from Nuclei Having Large Angular Momenta\*

J. ROBB GROVER

*Chemistry Department, Brookhaven National Laboratory, Upton, New York*

AND

JACOB GILAT†

*Chemistry Department, State University of New York at Stony Brook, Stony Brook, New York and  
Chemistry Department, Brookhaven National Laboratory, Upton, New York*

(Received 29 July 1966)

The statistical theory of nuclear de-excitation predicts  $\alpha$ -particle energy spectra having important features that were missed in earlier, less complete calculations. To a good approximation, the  $\alpha$  spectrum is composed of three qualitatively different subspectra. For  $\text{Dy}^{156*}$  compound nuclei formed by  $\text{Ce}^{140} + \text{O}^{16}$  at 90 MeV (lab), these subspectra have their respective maxima at 17, 12, and 7.5 MeV. The 7.5-MeV subspectrum should be resolvable into a group of sharp lines. The crucial roles of the lowest excited state at every angular momentum (the yrast levels), and of the competition with neutron and with dipole and quadrupole  $\gamma$ -ray emission, are stressed. Simple formulas are derived for estimating the energies at the maxima of the two lowest-energy subspectra. Since the  $\alpha$ -particle subspectra are predictions of the most widely used version of the statistical model of nuclear de-excitation, a failure to observe them would be important. If they are observed, the experimental data should provide information about several nuclear properties heretofore inaccessible.

### INTRODUCTION

**N**UCLEAR reactions in which  $\alpha$  particles are emitted with unexpectedly large probability at energies well below the Coulomb barrier have been observed.<sup>1-7</sup> Explanations for this phenomenon have

included suggestions that the emitting nuclei are non-spherical,<sup>2,5,8,9</sup> that the Coulomb barrier decreases with increasing excitation energy,<sup>6,10</sup> that the Coulomb barrier may be perturbed by intense localized heating over a small volume of the nucleus,<sup>7</sup> that localized heating may cause a local expansion of nuclear matter to a large radius before particle emission,<sup>11</sup> that alphas may be emitted to an important extent from the products of high-energy fission,<sup>7</sup> and that such alphas are emitted from nuclei excited to energies less than nucleon binding energies, but greater than alpha binding energies.<sup>12</sup> In carrying through the calculations for the statistical theory of nuclear de-excitation more completely than has been done previously, we find that sub-barrier  $\alpha$  particles are predicted without making special assumptions about nuclear shapes, etc. (see Fig. 6), partly by the simple process described in the last of the explanations cited above, but much more importantly, when the same nuclei possess large angular momenta, in related processes in which the  $\alpha$  particles

\* Research performed in part under the auspices of the U. S. Atomic Energy Commission.

† Present address: Israel Atomic Energy Commission, Soreq Nuclear Research Center, Yavne, Israel.

<sup>1</sup> M. Lefort, J. P. Cohen, H. Dubost, and X. Tarrago, *Phys. Rev.* **139**, B1500 (1965).

<sup>2</sup> H. Dubost, M. Lefort, J. Peter, and X. Tarrago, *Phys. Rev.* **136**, B1618 (1964).

<sup>3</sup> J. Muto, H. Itoh, K. Okano, N. Shiomi, K. Fukuda, Y. Omori, and M. Kihara, *Nucl. Phys.* **47**, 19 (1963).

<sup>4</sup> H. C. Britt and A. R. Quinton, *Phys. Rev.* **124**, 877 (1961).

<sup>5</sup> W. J. Knox, A. R. Quinton, and C. E. Anderson, *Phys. Rev.* **120**, 2120 (1960).

<sup>6</sup> C. B. Fulmer and C. D. Goodman, *Phys. Rev.* **117**, 1339 (1960).

<sup>7</sup> J. B. Harding, S. Lattimore, and D. H. Perkins, *Proc. Roy. Soc. (London)* **A196**, 325 (1949). See also Refs. 16 and 17 for additional references to relevant work done at about this time. This paper on cosmic-ray stars in emulsion is cited because the data it reports inspired ideas about how sub-barrier  $\alpha$ -particle emission might be explained. On the basis of more recent measurements, however, the "sub-barrier"  $\alpha$ 's seen in GeV proton irradiations of AgBr emulsions are convincingly explained as merely  $\alpha$ 's that are evaporated in the backward direction from recoiling excited nuclei. See E. W. Baker, S. Katcoff, and C. P. Baker, *Phys. Rev.* **117**, 1352 (1960); N. T. Porile, *Phys. Rev.* **135**, B371 (1964).

<sup>8</sup> R. Beringer and W. J. Knox, *Phys. Rev.* **121**, 1195 (1961).

<sup>9</sup> D. V. Reames, *Phys. Rev.* **137**, B332 (1965).

<sup>10</sup> E. Bagge, *Ann. Physik.* **33**, 389 (1938).

<sup>11</sup> T. Miyazima, K. Nakamura, and Y. Futami, *Progr. Theoret. Phys. (Kyoto)*, Suppl. 621 (1965).

<sup>12</sup> D. W. Lang, *Phys. Rev.* **123**, 265 (1961).

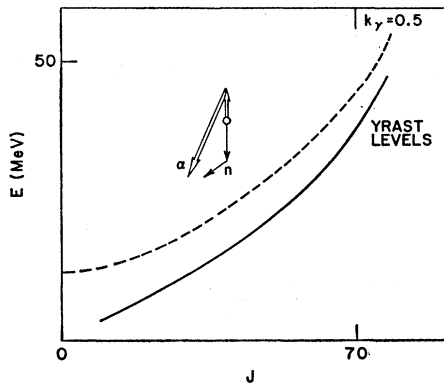


FIG. 1. Schematic diagram illustrating relative properties of  $\alpha$ -particle (double arrows) and neutron (single arrows) emission in nuclei for which  $B_\alpha < 0$  and  $B_n > 0$ . The fact that, on the average, the  $\alpha$ -particle can carry away more angular momentum than the neutron is emphasized.

are emitted at excitation energies well in excess of nucleon binding energies.

In the next section we describe those features of the nuclear-de-excitation process that cause the sub-barrier  $\alpha$ -particle emission to be enhanced at large angular momenta. We try to give enough insights to allow qualitative predictions to be made for other cases. Our discussion is guided and illustrated by the detailed results we obtained in our calculation for the system  $\text{Ce}^{140} + 0^{16}$  at 90 MeV (lab). Details of this calculation and other results can be obtained from the companion papers.<sup>13,14</sup>

In the last section, we derive an equation useful for quick estimates of the energies near which the most intense sub-barrier  $\alpha$ -particle emissions may be expected.

## DISCUSSION

We illustrate our remarks here with schematic diagrams such as Fig. 1, similar to those used in Ref. 14. The angular momentum of the nucleus is measured along the abscissa, and the excitation energy along the ordinate. The approximate locus of the lowest excited level at every angular momentum, called here the "yrast" levels,<sup>15</sup> is indicated by a solid line; in the schematic diagram this line is used for both the emitting nucleus and the emission product. The dashed line labeled  $k_\gamma = 0.5$  gives the approximate locus for which the nucleus has a 50% chance to decay by  $\gamma$  radiation.<sup>14</sup> The notation used here is the same as in Ref. 13 and 14. The region of the diagram enclosed between the dashed line and the yrast line is called the " $\gamma$ -cascade band" in the following discussion.

<sup>13</sup> J. R. Grover and J. Gilat, second preceding paper, Phys. Rev. **157**, 802 (1967).

<sup>14</sup> J. R. Grover and J. Gilat, first preceding paper, Phys. Rev. **157**, 814 (1967).

<sup>15</sup> J. R. Grover, following paper, Phys. Rev. **157**, 832 (1967).

The binding energy of an  $\alpha$  particle is negative, and of a neutron is positive, for all of the nuclei involved in our example system. In a diagram such as Fig. 1 (see also Fig. 7), the vertical binding-energy arrow for  $\alpha$  emission therefore points upward, and terminates at a higher energy than the downward-pointing binding-energy arrow for neutron emission from the same point. Since the  $\alpha$  particle is more massive than a neutron, it can carry away angular momentum more easily than can a neutron of the same energy. In addition, due to Coulomb effects, an  $\alpha$  particle is, on the average, emitted with greater energy than a neutron. This is illustrated by the angled kinetic-energy arrows connected to the points of the binding-energy arrows in Fig. 1. These differences between neutrons and  $\alpha$  particles should give rise to a region where  $\alpha$ -particle emission is faster than neutron emission. In our calculated example, we find that such a region occurs, and, indeed, that  $\alpha$ -particle emission is faster than neutron emission over almost the entire width of the  $\gamma$ -cascade band (see Fig. 2). Here,  $k_i(E, J) = \langle \Gamma_i(E, J) \rangle / \langle \Gamma_{\text{total}}(E, J) \rangle \approx \langle \Gamma_i(E, J) / \Gamma_{\text{total}}(E, J) \rangle$ , where  $\langle \Gamma_i(E, J) \rangle$  is the average emission width for emitting particle  $i$  (which may be a photon) from the nucleus at excitation energy  $E$  and angular momentum  $J$ , and  $\langle \Gamma_{\text{total}}(E, J) \rangle = \sum_i \langle \Gamma_i(E, J) \rangle$  summed over all species  $i$  which can be emitted.

Figure 2 exhibits an even more interesting feature. For energies at which the relative emission probability

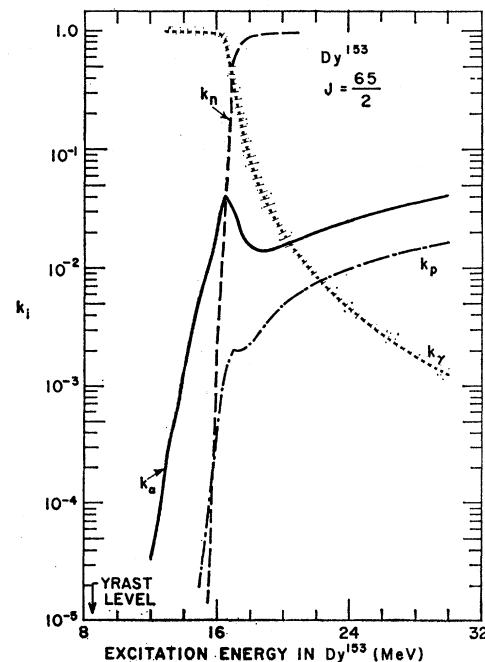


FIG. 2. Comparison of fraction of excited  $\text{Dy}^{153}$  nuclei which emit  $\alpha$  particles, neutrons, protons, and  $\gamma$  rays. The value of  $J$  is held constant at  $J = 65/2$ .

begins to decrease very steeply with decreasing excitation energy, the relative  $\alpha$ -particle emission probability goes through a pronounced maximum. Qualitatively, the appearance of this maximum is easily understood in terms of two effects: (1) For equal energies and orbital angular momenta, the centrifugal barrier is a greater obstacle to the neutron than it is to the more massive  $\alpha$  particle; (2) the smallest kinetic energy at which the neutron can be emitted is zero, a "hard" absolute limit, while the lowest-energy  $\alpha$  particles are limited by the relatively "soft" Coulomb barrier. The  $\alpha$ -particle emission rate therefore does not exhibit as steep a drop with decreasing excitation energy as does that of the neutrons, for energies less than that at which  $k_\gamma=0.5$ . The corresponding emission rate for  $\gamma$  rays falls even less steeply. Now, in our example (Fig. 2), the fraction of the nuclei de-exciting themselves by neutron emission (i.e.,  $k_n$ ) passes rather quickly from nearly unity to values of order  $10^{-3}$ , in decreasing the nuclear excitation energy by only 2 MeV, from 18 to 16 MeV. Across this short energy interval, where forms of nuclear de-excitation other than neutron emission begin to account for most of the de-excitation, the relative emission probability of  $\alpha$  particles must rise if there are no overriding effects. Such an overriding effect could come about if the absolute  $\gamma$  emission rate were to rise steeply enough to compensate for the drop in the neutron emission rate; but, as we can see intuitively, the  $\gamma$  emission rate should decrease relatively

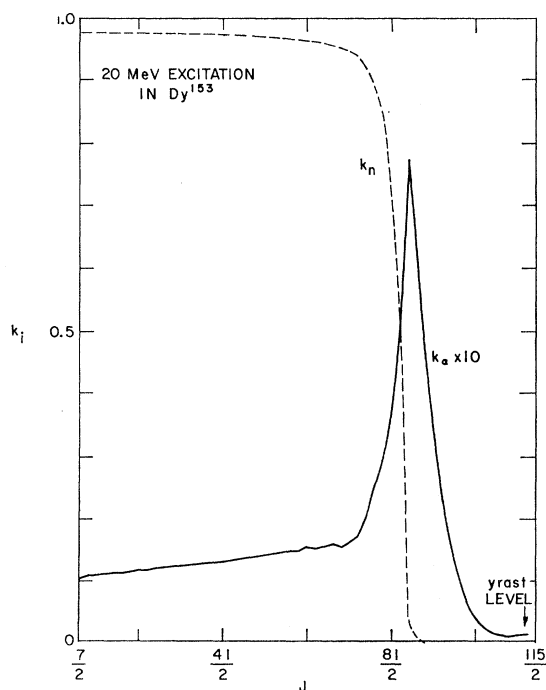


FIG. 3. Fraction of  $Dy^{153}$  nuclei excited to 20 MeV which emit  $\alpha$  particles and neutrons, as a function of angular momentum.

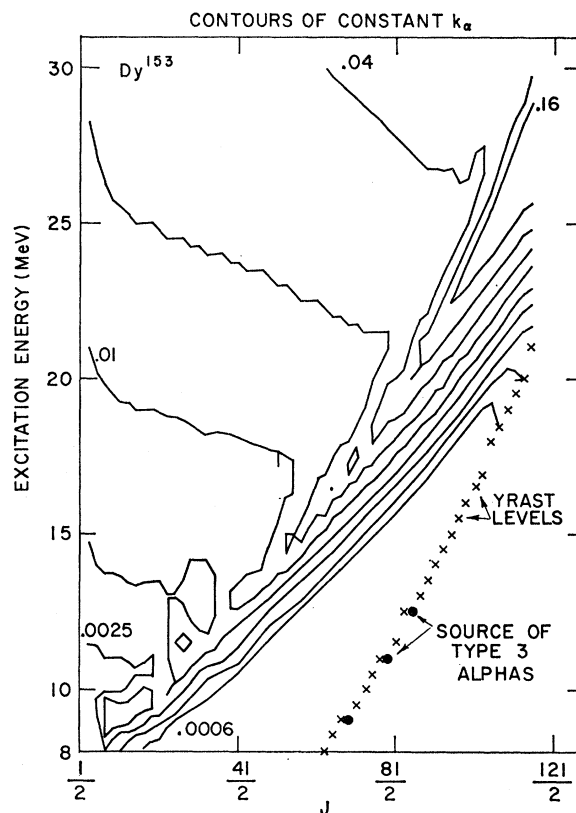


FIG. 4. Contour diagram of  $k_\alpha$  in  $Dy^{153}$ . Neighboring contours differ by a factor of 2. The X's give the position on the energy grid next above the yrast level at each angular momentum. Grid positions from which dipole  $\gamma$ -ray emission cannot occur are indicated by solid circles.

slowly in this region, instead. Since the  $\alpha$ -particle emission rate is falling more steeply than the  $\gamma$ -ray emission rate, with decreasing energy, the relative emission probability of  $\alpha$  particles must eventually turn downward again, and will therefore pass through a maximum. Thus, a maximum in  $k_\alpha$  near the excitation energy at which  $k_\gamma=0.5$  is to be expected when neutron emission passes from dominance to insignificance over a narrow interval of excitation energy.

This behavior of  $k_\alpha$  is the high angular-momentum analog of charged-particle emission below or near the neutron-emission threshold, e.g., of slow proton<sup>16-21</sup> and  $\alpha$ <sup>6,12</sup> emission, long-range  $\alpha$ -particle emission from excited states populated in radioactive-decay proc-

<sup>16</sup> Y. Fujimoto and Y. Yamaguchi, Progr. Theoret. Phys. (Kyoto) 3, 462 (1948); Phys. Rev. 75, 1776 (1949); Progr. Theor. Phys. (Kyoto) 4, 468 (1949).

<sup>17</sup> K. J. Le Couteur, Proc. Phys. Soc. (London) A63, 259 (1950).

<sup>18</sup> G. Rudstam, thesis, Uppsala University, 1956 (unpublished).

<sup>19</sup> D. L. Allen, Nucl. Phys. 6, 464 (1958).

<sup>20</sup> N. O. Lassen and V. A. Sidorov, Nucl. Phys. 19, 579 (1960).

<sup>21</sup> J. Delorme, Nucl. Phys. 47, 544 (1963).

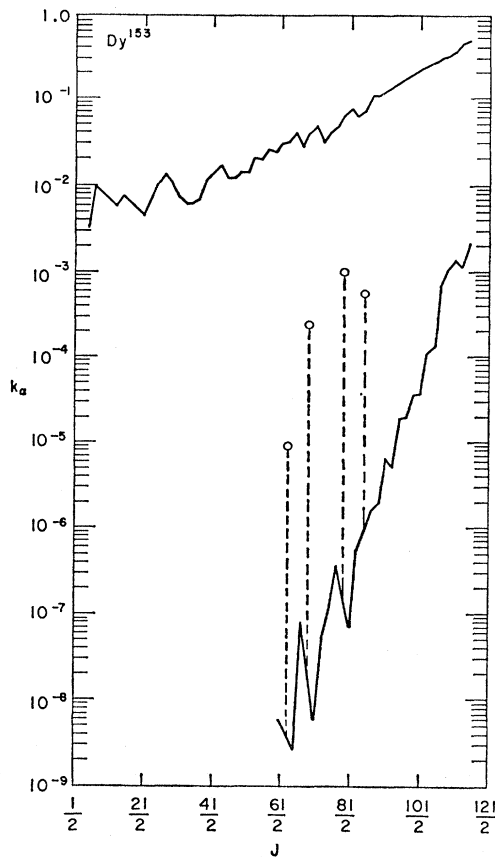


FIG. 5. Values of  $k_\alpha$  at the maximum, for each angular momentum, compared with values of  $k_\alpha$  at the energy-grid positions next above the yrast levels, for  $\text{Dy}^{153}$ . The open circles are the values of  $k_\alpha$  at the grid positions for which dipole  $\gamma$ -ray emission cannot occur, and thus represent competition mainly between  $\alpha$ -particle emission and quadrupole  $\gamma$ -ray emission. The vertical dashed lines just indicate approximately what these values would have been had dipole  $\gamma$ -ray emission been possible.

esses,<sup>22</sup> thermal-neutron-induced  $n, \alpha$  reactions,<sup>23-26</sup> etc. Here, the neutron threshold is effectively determined by the yrast levels, rather than by only the ground state.

Dudey and Sugihara,<sup>27</sup> and Reames<sup>9</sup> have reported, on the basis of less complete calculations than ours, that one might expect a relative enhancement of  $\alpha$ -particle emission over neutron and proton emission, as

<sup>22</sup> For an account of long-range  $\alpha$ -particle emission and a directory to the literature, see E. K. Hyde, I. Perlman, and G. T. Seaborg, *The Nuclear Properties of the Heavy Elements, II, Detailed Radioactivity Properties* (Prentice-Hall, Inc., Englewood Cliffs, New Jersey, 1964), p. 462, ff.

<sup>23</sup> R. D. Griffioen and J. O. Rasmussen, University of California Radiation Laboratory Report No. UCRL-9566, 1961 (unpublished), p. 147.

<sup>24</sup> E. Cheifetz, J. Gilat, A. I. Yavin, and S. G. Cohen, *Phys. Letters* **1**, 289 (1962).

<sup>25</sup> R. D. Macfarlane and I. Almodovar, *Phys. Rev.* **127**, 1665 (1962).

<sup>26</sup> V. N. Andreev and S. M. Sirotkin, *Yadernaya. Fiz.* **1**, 252 (1965) [English transl.: *Soviet J. Nucl. Phys.* **1**, 177 (1965)].

<sup>27</sup> N. D. Dudey and T. T. Sugihara, *Phys. Rev.* **139**, B896 (1965).

a result of the difference in binding energies between  $\alpha$ 's and nucleons, together with more effective suppression of the latter by the centrifugal barrier. Although they did not take into account the important competitive emission of  $\gamma$  rays, our results confirm their qualitative conclusion quite well.

The relationship between  $k_\alpha$  and  $k_n$  as a function of angular momentum, at a constant excitation energy of 20 MeV, is exhibited in Fig. 3. On the linear ordinate scale of this plot, the relative magnitude of the maximum in  $k_\alpha$  can be seen more clearly.

To examine the behavior of  $k_\alpha$  over a large part of the  $E$ -versus- $J$  plane, it is useful to prepare contour plots, such as that of Fig. 4. Here, a contour line represents a locus of constant  $k_\alpha$ , each line being a factor of 2 greater or less than its immediate neighbors. This figure displays the relationship between the excitation energy at which the maximum of  $k_\alpha$  occurs, at constant angular momentum, and the corresponding yrast level at that angular momentum. The energy at this maximum is higher than the energy of the corresponding yrast level by about  $B_n$ , the neutron binding energy. Indeed, the locus of maxima in  $k_\alpha$  in the  $E$ - $J$  plane is nearly the same as the locus for which  $k_\gamma=0.5$ , as would be expected from the qualitative analysis offered above. Above the "mountain range" formed by these maxima in  $k_\alpha$  is a broad plain, rising relatively gently from lower left to upper right. Below the mountain range the  $k_\alpha$  surface decreases very steeply.

For a given angular momentum, the value of  $k_\alpha$  at the yrast level itself is usually much smaller than it is at the maximum, as shown in Fig. 5. Notice that the former values of  $k_\alpha$  rise much more steeply with increasing angular momentum than do the latter values. Moreover, for a few of the yrast levels the values of  $k_\alpha$  are calculated to be several orders of magnitude larger than for their neighbors. These special levels and their corresponding values of  $k_\alpha$  are designated in Fig. 5 by the open circles and dashed lines, and in Fig. 4 by the closed circles. We see that these are the very levels already identified<sup>14</sup> as those for which dipole  $\gamma$ -ray emission is not possible. For these yrast levels, the alpha particles are emitted in competition essentially only with quadrupole  $\gamma$ -ray emission. Thus the values of  $k_\alpha$  for these levels are larger than for the neighboring values for which dipole  $\gamma$ -ray emission is possible by a factor which is comparable with the ratio of the reduced dipole  $\gamma$ -ray emission rate to the reduced quadrupole  $\gamma$ -ray emission rate. As already stated in Ref. 13, this ratio is assumed to be roughly  $10^8$  in our calculation.

Broadly speaking, we may therefore distinguish three regions of the  $E$ -versus- $J$  plane of an excited nucleus in terms of the outstanding features of the values of  $k_\alpha$ . Moreover, we have explained in the foregoing remarks the relationship between these three regions and the three regions distinguished in our discussion of the  $\gamma$ -ray emission.<sup>14</sup> Each of the three regions contributes its own distinctive  $\alpha$ -particle subspectrum to the over-

all  $\alpha$ -particle energy spectrum. These subspectra are described in the following paragraphs.

The broad plain represented by the upper-left portion of Fig. 4 is associated with a spectrum in which the maximum differential (per unit energy) alpha-particle emission rates occur for kinetic energies near the Coulomb barrier (17–18 MeV in this example), the rates falling steeply at lower energies because of inhibition by the Coulomb barrier, and being governed at the higher energies mainly by the energy dependences of the level densities of the  $\alpha$ -particle emission products. This subspectrum is, indeed, approximately the same as the spectrum that would be calculated ignoring competitive  $\gamma$ -ray emission and other effects associated with the conservation of angular momentum. We call this subspectrum, for convenience, the *type-I*  $\alpha$ -particle subspectrum; the other two subspectra we call *type II* and *type III*, respectively. In our example calculation, the  $\alpha$ -particle spectra emitted from Dy<sup>156</sup>, Dy<sup>155</sup>, and Dy<sup>154</sup> are composed almost entirely of the type-I subspectra we have just described. Spectra for Dy<sup>156</sup> and Dy<sup>154</sup> are shown in Fig. 6.

The region including the maxima in the values of  $k_\alpha$ , i.e., the “mountain range,” is associated with the type-II subspectrum, the maximum of which occurs at a kinetic energy near 12 MeV. This energy is well below the Coulomb barrier. Below 12 MeV, the type-II subspectrum drops very steeply, being under the influence of a formidable Coulomb barrier, and above 12 MeV it drops relatively faster than does the type-I  $\alpha$ -particle subspectrum, for energies above its own maximum. Thus the type-II subspectrum is not as wide as the type-I subspectrum. The reasons for the steep decrease on the high-energy side of the type-II subspectrum are explained further on. The reason the maximum emission rate occurs near 12 MeV can be understood from a knowledge of the relevant yrast levels, the binding energy of an  $\alpha$  particle to the emitting nucleus, and the energy by which the maximum in  $k_\alpha$  exceeds its corresponding yrast level. The interrelations of these quantities are displayed in the schematic diagram of Fig. 7.

Consider  $\alpha$ -particle emission from nuclei having excitation energy  $\bar{E}$  and angular momentum  $\bar{J}$ , represented by the open circle. We have placed this open circle just below the line representing the locus of energy-spin combinations for which  $k_\gamma=0.5$ , because we know that, in our calculation, this is where the maximum in  $k_\alpha$  occurs. Assuming that the binding energy of an  $\alpha$  particle,  $B_\alpha$ , is negative, we draw the binding-energy arrow pointing upward. Now, if the  $\alpha$  particle carried off no angular momentum in its emission, its kinetic arrow would point straight down, and it could be emitted with no more kinetic energy than would allow it to populate that yrast level in the product which has angular momentum  $\bar{J}$ . We further assume, as is also implied by the diagram, that the yrast level at spin  $J$  in the product has nearly the same

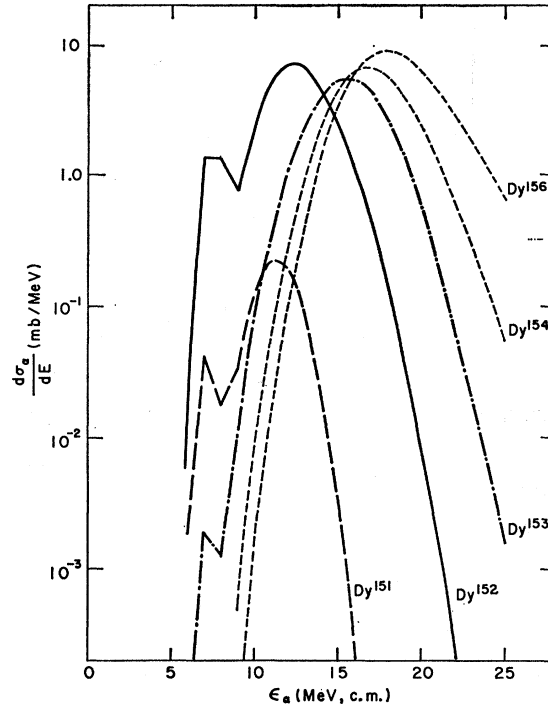


FIG. 6. Calculated  $\alpha$ -particle spectra for several nuclei in the chain of neutron emissions in the decay of excited Dy<sup>156</sup> considered in the sample calculation. The population distribution of excited nuclei with respect to energy and angular momentum can be seen in a companion paper (Ref. 14).

energy  $E_{J'}$  as the energy  $E_J$  of the yrast level of spin  $J$  in the emitting nucleus; i.e., we assume that  $E_{J'} \approx E_J$ . The maximum energy with which an alpha particle could be emitted and carry off no angular momentum is thus

$$\epsilon \approx -B_\alpha + (\bar{E} - E_{J'}) \approx -B_\alpha + B_n, \quad (1)$$

where we take advantage of our observation that in our example  $\bar{E} - E_J \approx B_n$ .<sup>14</sup> It should be noted that the latter approximation is useful only when neutron emission dominates the nuclear de-excitation above energies for which  $k_\gamma=0.5$ . As shown in the diagram,  $\alpha$  particles may have greater kinetic energy than given by Eq. (1), if they are emitted with orbital angular momentum, allowing the point of the kinetic arrow to be displaced to lower angular momenta. If the Coulomb barrier is much larger than the  $\alpha$ -particle energy, then emission of  $\alpha$  particles with orbital angular momentum will be preferred. On the other hand, the centrifugal barrier slows the emission of  $\alpha$  particles carrying angular momentum; the greater the orbital angular momentum, the more effective the retardation. The  $\alpha$ -particle emission will thus tend to proceed with that combination of energy and orbital angular momentum which allows the greatest emission rate, being limited at lower energies by the Coulomb barrier, and at higher energies (but lower values of  $J$ ) by the centrifugal barrier. The shape

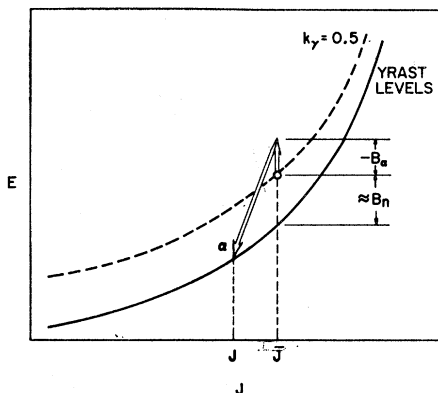


FIG. 7. Schematic diagram to illustrate derivation of Eq. (6b).

of the type-II subspectrum thus depends on the disposition in energy and angular momentum of the yrast levels of the alpha-emission product. We note in passing that this explains the steep decrease at energies above the maximum in the type-II subspectrum. A simple algebraic expression useful for estimating the energies at the maxima of type-II and type-III subspectra is given in the next section. For our present argument we merely point out that, according to Eq. (1), the energy at the maximum of the type-II  $\alpha$ -particle subspectrum should be not too much larger than  $-B_\alpha + B_n = 11.0$  MeV. Thus, the energy at the maximum of the type-II subspectrum is only 12 MeV, because the  $\alpha$  particles tend to be emitted with a relatively modest amount of orbital angular momentum. The appreciable relative probability for  $\alpha$ -particle emission at energies so far beneath the Coulomb barrier seems surprising, but, as we have explained, the  $\alpha$  particles associated with the type-II subspectrum are emitted mainly in competition with dipole  $\gamma$ -ray emission, rather than with the relatively much faster ( $s$ - and  $p$ -wave) neutron emission. Our calculated alpha-particle spectra of  $\text{Dy}^{151}$  and  $\text{Dy}^{152}$ , shown in Fig. 6, are predominantly composed of type-II subspectra.

Experimentally, we cannot yet distinguish between the  $\alpha$ -particle spectra associated with the successive species of the decay cascade of a compound nucleus, and only the total spectrum can be measured. The intensity of the type-I component of this spectrum should be roughly independent of angular-momentum considerations. As can be seen from Fig. 4, the value of  $k_\alpha$  at constant energy rises slowly with increasing angular momentum (see also Refs. 9 and 27). On the other hand, for a given initial energy, there are more chances for  $\alpha$  emission from nuclei of low angular momentum before they are de-excited to the vicinity of yrast. These two effects tend to cancel each other, and the over-all intensity remains approximately constant. The intensity of the type-II component does depend on angular-momentum effects. As shown in Figs. 4 and 5, the value of  $k_\alpha$  at its maximum in the Dy case rises steeply with increasing angular momentum, increasing

two orders of magnitude between  $J=1$  and  $J=58$ . This is due mainly to the increasing slope of the  $E_J$ -versus- $J$  curve. It can be estimated from Fig. 4 that, for  $\text{Dy}^{156}$  compound nuclei of low spin, the relative contribution of the type-II subspectrum would be only about 0.1 of what we calculated for our example system (for which the average angular momentum is  $30\hbar$ ), and would hardly be noticeable (see Fig. 3 of Ref. 13). In cases where the difference between successive yrast levels increases less steeply with increasing angular momentum, the situation will be quite different. Thus, measurement of the relative intensity of the type-II subspectrum as a function of angular momentum would provide information on the spin dependence of yrast-level energies.

Alpha particles emitted from yrast levels for which dipole  $\gamma$ -ray emission is not possible form the type-III subspectrum.<sup>28</sup> Here, in contrast to alpha-particle emission contributing to the type-II subspectrum, we have  $\bar{E} - E_J' = E_J - E_J' \approx 0$  and, by Eq. (1),  $\epsilon \approx -B_\alpha$  if the alpha particles are emitted with no orbital angular momentum. Again, we see the increased emission rate resulting from emission energy gained when emissions take place with orbital angular momentum. Although this is a relatively small effect for emissions leading to type-II subspectra, it is clearly much more important for the type-III subspectra. Indeed, for our example, we find that the maximum emission rate occurs for  $\alpha$  particles emitted with orbital angular momenta near  $10\hbar$ , for which an additional 4 MeV in emission energy is realized. The maximum of the type-III subspectrum then falls at  $-B_\alpha + 4 = 7.5$  MeV.<sup>29</sup>

<sup>28</sup> Alpha-particle emission from the high-spin isomer of  $\text{Po}^{212}$  is a famous example of this. See I. Perlman, F. Asaro, A. Ghiorso, A. Larsh, and R. Latimer, *Phys. Rev.* **127**, 917 (1962).

<sup>29</sup> The skeptical reader can easily verify independently of our calculation that  $\alpha$ -particle emission from certain yrast levels in  $\text{Dy}^{153}$  may well proceed with rates of order  $10^{-5}$  to  $10^{-3}$  as fast as quadrupole radiation from the same levels. Assuming that the quadrupole radiations can only proceed through one 0.5-MeV transition, single-particle estimates [S. A. Moszkowski, in *Alpha-, Beta-, and Gamma-Ray Spectroscopy*, edited by K. Siegbahn (North Holland Publishing Company, Amsterdam, 1965), p. 863] give half lives of  $2 \times 10^{-10}$  and  $6 \times 10^{-9}$  sec, respectively, for  $E2$  and  $M2$  radiation. If we assume that the yrast levels are given approximately by the rotational energy calculated as if the  $\text{Dy}^{153}$  nucleus were a rigid sphere, with  $r_0 = 1.2 \times 10^{-13}$  cm, then a 7.3-MeV alpha particle will carry away about 8 units of orbital angular momentum (remembering that 3.2 MeV of the 7.3 MeV comes from the negative alpha-particle binding energy). Using Eq. (8-6) on p. 226 of Ref. 32, the half-life of  $\alpha$ -particle emission with no angular-momentum barrier is estimated to be  $6 \times 10^{-9}$  sec. The effect of angular momentum is conveniently estimated using an approximation suggested by J. O. Rasmussen [*Phys. Rev.* **115**, 1675 (1959)]. The result is a partial  $\alpha$ -decay half-life, to one single level, of  $2 \times 10^{-5}$  sec. Taking into account all the neighboring levels to which the  $\alpha$  decay must be considered, the total partial  $\alpha$ -emission half-life should be shorter than the one-level value by about an order of magnitude, say  $10^{-6}$  sec. This estimate is to be compared with the above  $\gamma$ -ray lifetimes, and verifies our qualitative result. It may be argued that the  $\alpha$ -particle emission may be hindered, but so, for that matter, may the gamma transition (Ref. 30), especially the  $M2$ . Experimental evidence that alpha-particle emission indeed sometimes competes effectively with dipole and quadrupole  $\gamma$ -ray emission may be found in Refs. 22-26.

Now, in general, there will probably not be many yrast levels from which  $\alpha$ -particle emission makes an important contribution to the type-III subspectrum. Moreover, the  $\alpha$  particles emitted from these levels will tend strongly to populate product levels which are yrast levels, or near yrast levels. Thus, the emitting levels are expected to be both (i) very narrow, and (ii) few in number, in any given system. The type-III subspectrum should be composed, then, of resolvable lines. From Fig. 5 we see that the values of  $k_\alpha$  at the special yrast levels responsible for the type-III subspectrum rise steeply with increasing energy. This rise reflects the increasingly steep average rise in energy of the yrast levels with increasing angular momentum.<sup>15</sup> The gain in energy realized by the  $\alpha$ -particle emitted with a given orbital angular momentum thereby increases with increasing angular momentum. This same increasingly steep rise, however, makes the occurrence of those yrast levels unable to decay by dipole emission progressively less likely as the angular momentum increases.<sup>15</sup> Thus, in our calculation, the contributions to the  $\alpha$ -particle type-III subspectrum are effectively confined to the region of angular momenta between  $J=20\hbar$  and  $40\hbar$ . Below  $20\hbar$ ,  $k_\alpha$  is too small. Above  $40\hbar$ , the special  $\alpha$ -particle-emitting yrast levels are unlikely to occur.

In our calculated example, there were no spectra comprised mostly of type-III subspectra. However, the 7–8-MeV energy of this subspectrum is so far below the energies of the type-I and type-II subspectra that the contributions of type-III subspectra are clearly seen as separate maxima in the calculated  $\alpha$ -particle spectra of Dy<sup>161</sup>, Dy<sup>162</sup>, and Dy<sup>163</sup> in Fig. 6. Since our calculation was performed with an imposed energy grid of 0.5 MeV, it does not, of course, reveal the decomposition of the 7.5-MeV peak into narrow lines.

From Figs. 4 and 5 it can be seen that for angular momenta of  $20\hbar$  to  $45\hbar$ , where most of the sub-barrier  $\alpha$  particles arise in our calculated example, the values of  $k_\alpha$  are still quite small, especially for the type-III subspectrum. Why, then, do these subspectra show up so prominently? The answer is that these regions of the nucleus are, at some point in the de-excitation process, very heavily populated, and this offsets the smallness of the branching ratios  $k_\alpha$ . Cascade  $\gamma$ -ray de-excitation plays a strong role in building up these high populations, especially for those yrast levels which emit  $\alpha$ -particles in the type-III subspectrum. However, it should be remembered that transitions from yrast level to yrast level may well be hindered compared to transitions to levels just above yrast levels, especially at the larger angular momenta,<sup>15</sup> and this could reduce the predicted intensity of type-III  $\alpha$  emissions. These matters are discussed more thoroughly in a companion paper, Ref. 15.

It should be noted that the intensity of the type-III  $\alpha$ -particle subspectrum depends crucially on the quadrupole  $\gamma$ -ray emission. Although we have chosen to use a rather slow rate in this calculation, it should be

remembered that we make no distinction between electric and magnetic transitions. Even if electric-quadrupole transitions are greatly speeded by collective effects, as they are known to be in many cases near the ground state, the magnetic-quadrupole transitions show no such pronounced enhancement, and tend instead to be retarded by factors comparable to the retardation factors for electric-dipole transitions.<sup>30</sup> In general, we must expect about half<sup>15</sup> the  $\alpha$  particles in the type-III subspectrum to be emitted in competition with magnetic-quadrupole radiation, so the qualitative conclusion of our sample calculation is unaffected.

Even if the quadrupole  $\gamma$ -ray emission rates are as much as 100 times faster than we have assumed, the type-III subspectrum should be observable because it consists of sharp lines (from Fig. 6 it is clear that even with a resolution of only 0.5 MeV, the type-III subspectrum could be seen at  $\frac{1}{10}$  the relative intensity shown in the figure, while 50-keV resolution should be attainable).

Angular distribution experiments on the type-II and type-III subspectra should be useful in verifying that they indeed originate in the predicted way, and to measure some nuclear properties. Since the  $\alpha$  particles in both subspectra carry away considerable angular momentum, they should be most intense near  $0^\circ$  and  $180^\circ$  with respect to the incident beam, but symmetric about  $90^\circ$  in the c.m. system. However, the quadrupole transitions competing with the  $\alpha$  particles in the type-III subspectrum may be so slow<sup>29</sup> that the angular distribution washes out due to thermal relaxation of the polarized nuclei. This should not affect the type-II spectrum whose  $\alpha$  particles compete with much faster dipole radiation. Note that the residual nuclei emitting  $\alpha$  particles in the type-III subspectrum should stop moving before  $\alpha$  emission if they are allowed to penetrate a solid catcher material. If they are not stopped, they could recoil a considerable distance before emitting the  $\alpha$  particle (of order 1 cm for magnetic-quadrupole radiation, and farther if the radiation is retarded).

If type-III-sub-spectrum lines can be observed, they should be very useful for mapping out the yrast levels. The nucleus from which  $\alpha$  particles of a given line are emitted can be identified by standard means, e.g., by use of excitation functions and of "cross bombardments." Judicious use of different target-projectile combinations to excite the lines will then give an approximate measure of the angular momentum of the emitting level, because each target-projectile combination will provide compound nuclei with a characteristic population distribution in angular momentum, which can be at least approximately calculated. The excitation function of the line will then provide an estimate of the excitation energy of the emitting state. In favorable cases, this could probably be checked by measurements of the  $\gamma$  rays in prompt coincidence with

<sup>30</sup> D. H. Wilkinson, in *Nuclear Spectroscopy: Part B*, edited by F. Ajzenberg-Selove (Academic Press, New York, 1960), p. 852.

the  $\alpha$  particles. In general, one expects a family of several such lines to be associated with any given emitting level, and the energies of the most intense lines should give an approximate measure of the orbital angular momentum carried away by the  $\alpha$  particles [see Eq. (6b) of the following section]; i.e., if the energy and angular momentum of the emitting yrast level is known, then the energy and angular momentum of the product yrast levels can also be estimated, and *vice versa*.

#### ESTIMATION OF ENERGIES AT MAXIMA OF TYPE-II AND TYPE-III SUBSPECTRA

At this point, we derive a formula for estimating the  $\alpha$ -particle energies at the maxima of the type-II and type-III subspectra. From Eqs. (11) and (13) of Ref. 13 we see that for a given emitting level, of energy and spin  $\bar{E}\bar{J}$ , the dependence of the  $\alpha$ -particle emission rate on kinetic energy and orbital angular momentum  $l$  is contained in the transmission coefficients  $T_l(\epsilon)$ , and the product level density  $\omega(EJ)$ . The product levels populated most heavily by  $\alpha$ -particle emission at energies well below the Coulomb barrier are the yrast levels and the levels nearest the yrast levels. This is because the transmission coefficients are rising very steeply indeed with increasing energy (see Fig. 7). To a first approximation, therefore, the level-density factor can be treated as being roughly constant in the region of preferred product formation, i.e., along the yrast line. With the constraint between the kinetic energy and the angular momentum of the product levels to which the alpha particle can be emitted at that energy, we have

$$(\bar{J}-J)\bar{E}_J \approx \epsilon - (\bar{E} - B_\alpha - E_J), \quad (2)$$

where  $\bar{E}_J = \langle E_J - E_{J-1} \rangle$ , the average being taken over the yrast-level energies in the interval from  $J$  to  $\bar{J}$ . We assume that in the angular momentum interval of interest,<sup>15</sup>  $\bar{E}_J > 0$ . Since the most heavily populated product levels are confined within a few adjacent values of  $J$ , we use the approximation

$$\sum_{l=L}^{\infty} T_l \propto T_L, \quad (3)$$

where  $L = \bar{J} - J$ . The energy at the maximum of the sub-spectrum is the energy at which  $dR_{\mu\alpha}(\bar{E}\bar{J}; EJ)/dE = 0$ , subject to the constraint of Eq. (2); for convenience, we treat angular momentum as a continuous variable. When  $\omega(EJ)$  is assumed constant, we see from Eqs. (3) and (11) of Ref. 13 that the maximum in  $R_{\mu\alpha}(\bar{E}\bar{J}; EJ)$  occurs at the same energy as the maximum in  $T_L(\epsilon)$ . For our purpose, it is a sufficiently good approximation to take  $T_L(\epsilon)$  proportional to the angular-momentum-dependent penetrability,

$$T_L(\epsilon) \propto P(\epsilon, L) \approx p(\epsilon)q(L).$$

We use for the energy-dependent factor the simple form given by Bethe<sup>31</sup> and others<sup>32</sup> and for the angular-momentum-dependent factor the approximation suggested by Perlman and Rasmussen,<sup>33</sup> to obtain

$$T_L(\epsilon) \propto \exp \left\{ -2^{3/2} \hbar^{-1} \mu^{1/2} Zze^2 \epsilon^{-1/2} \right. \\ \left. \times \left[ \cos^{-1} \left( \frac{\epsilon}{\mathfrak{B}} \right)^{1/2} - \left( \frac{\epsilon}{\mathfrak{B}} \right)^{1/2} \left( 1 - \frac{\epsilon}{\mathfrak{B}} \right)^{1/2} \right] \right. \\ \left. - \hbar^{2^{1/2}} [Zze^2 \mu R]^{-1/2} [L + \frac{1}{2}]^2 \right\}. \quad (4)$$

Here,  $\mu = mM/(m+M)$ , where  $m$  and  $M$  are the masses of the emitted particle and emission product, respectively,  $z$  and  $Z$  being their respective atomic numbers. The unit charge is given by  $e$ , the nuclear radius by  $R = (1.30A^{1/3} + 1.20) \times 10^{-13}$  cm, and a "Coulomb barrier" by  $\mathfrak{B} = Zze^2/R$ . In the range of values of  $\epsilon/\mathfrak{B}$  of relevance for type-II and type-III  $\alpha$ -particle subspectra, Eq. (4) is conveniently simplified by the approximation

$$\epsilon^{-1/2} \left[ \cos^{-1} \left( \frac{\epsilon}{\mathfrak{B}} \right)^{1/2} - \left( \frac{\epsilon}{\mathfrak{B}} \right)^{1/2} \left( 1 - \frac{\epsilon}{\mathfrak{B}} \right)^{1/2} \right] \propto \epsilon^{-2}. \quad (5)$$

With the help of Eq. (5), and applying Eq. (2), one sees that  $dT_L(\epsilon)/dE = 0$  at energy  $\epsilon_m$ , which is a solution of the quartic equation

$$\epsilon_m^3 (\epsilon_m - \bar{E} + B_\alpha + E_J + \bar{E}_J/2) = 0.019 \mu z ZR^{1/2} \bar{E}_J^2 \mathfrak{B}^2, \quad (6a)$$

where energies are in MeV,  $\mu$  is in mass numbers, and  $R$  is in F. The relevance of the quantity  $\bar{E} - B_\alpha - E_J$  in the substitution for  $L$  may be readily understood from Fig. 7. Numerical evaluation of Eq. (6a) gives roughly correct results, compared to the more detailed evaluation,<sup>18</sup> but we find that the results are more accurate if the numerical constant is increased to 0.04.

$$\epsilon_m^3 (\epsilon_m - \bar{E} + B_\alpha + E_J + \bar{E}_J/2) = 0.04 \mu z ZR^{1/2} \bar{E}_J^2 \mathfrak{B}^2. \quad (6b)$$

The difficulty seems mainly due to the roughness of the approximation in the  $L$ -dependent part of Eq. (4).

For the type-II subspectrum, whenever the substitution  $\bar{E} - E_J \approx B_n$  is appropriate, we see that usually  $[\epsilon_m - (B_n - B_\alpha) + \bar{E}_J/2] \ll \epsilon_m$ , and an approximate solution of Eq. (6b) is

$$\epsilon_m(\text{type II}) = 0.04 \mu z ZR^{1/2} \mathfrak{B}^2 \bar{E}_J^2 (B_n - B_\alpha - \bar{E}_J/2)^{-3} \\ + (B_n - B_\alpha - \bar{E}_J/2). \quad (7)$$

<sup>31</sup> H. A. Bethe, Rev. Mod. Phys. 9, 161 (1937).

<sup>32</sup> G. Friedlander, J. Kennedy, and J. M. Miller, *Nuclear and Radiochemistry* (John Wiley & Sons, New York, 1964). See especially Eqs. (8-2) and (8-5) on pp. 225 and 226.

<sup>33</sup> I. Perlman and J. O. Rasmussen, in *Handbuch der Physik*, edited by H. Geiger and K. Scheel (Julius Springer Verlag, Berlin, 1957), Vol. 42, p. 149.



For the type-III subspectrum, for which  $\bar{E} - E_{\bar{J}} \approx 0$ , so that  $\epsilon_m \gg -B_\alpha$ , an approximate solution of Eq. (6b) is

$$\epsilon_m(\text{type III}) = [0.04\mu z Z R^{1/2} \mathcal{Q}^2 \dot{E}_J^2]^{1/4} + \frac{1}{4}(-B_\alpha - \dot{E}_J/2). \quad (8)$$

Eqs. (7) and (8) give convenient starting points for a trial-and-error solution of Eq. (6b). As we explained in the preceding section, the most important contributions to the type-II and type-III subspectra are made by excited nuclei within a limited range of angular momenta, in most practical situations. In addition, it can be seen from Eqs. (7) and (8) that the dependence of  $\epsilon_m$  on  $\dot{E}_J$  is quite weak [in Eq. (7) the first term on the right is much smaller than the second term, while in Eq. (8) the dominant first term is proportional to  $(\dot{E}_J)^{1/2}$ ], while the dependence of  $\dot{E}_J$  itself on  $J$  is usually weaker<sup>15</sup> than  $\dot{E}_J \propto J$ . Furthermore, the dependence of  $\epsilon_m$  on  $\bar{J}$  enters essentially only through  $\dot{E}_J$ . Thus, the application of Eq. (6b) at those values of  $\bar{J}$  representing nuclei making the most important contributions to the type-II and type-III subspectra should suffice for useful predictions of  $\epsilon_m$ . For the de-excitation of Dy<sup>152</sup> in our sample calculation, appropriate values to use are  $\bar{J}=30$  (for which  $\dot{E}_J \approx 0.41$  MeV) for the type-II subspectrum, and  $\bar{J}=20$  (for which  $\dot{E}_J \approx 0.25$  MeV) for type III.

A rough estimate of the average amount of angular momentum removed by those  $\alpha$  particles contributing to the type-II and type-III subspectra is obtained from Eq. (2):

$$\langle \bar{J} - J \rangle \approx (\epsilon_m - \bar{E} + B_\alpha + E_{\bar{J}}) / \dot{E}_J.$$

In connection with the  $\alpha$ -particle spectrum measured<sup>4</sup> for the system C<sup>12</sup>+Au<sup>197</sup>, at 126 MeV, we assume that the nuclei emitting  $\alpha$  particles which would contribute to the type-II and type-III subspectra would be near At<sup>202</sup>. For this nuclide,  $B_n \approx 8.09$  MeV<sup>34</sup> and  $B_\alpha = -6.36$  MeV.<sup>35</sup> The average angular momentum of the emitting nuclei is roughly<sup>36</sup>  $\langle \bar{J} \rangle \approx 45$ . Estimating that

$$E_J \approx E(\text{rotation}) = [\hbar^2 / (2g)] J(J+1),$$

where  $g = \frac{2}{5}MR^2$ , we obtain

$$\dot{E}_J \approx (\hbar^2/g) J_{\text{av}}, \quad (9)$$

where  $J_{\text{av}}$  is taken to be midway between  $\langle \bar{J} \rangle$  and the average angular momentum of the product of alpha-particle emission. With  $R = 1.2A^{1/3} \times 10^{-13}$  cm, we obtain, for  $J_{\text{av}} = 40$ , the value  $\dot{E}_J \approx 0.43$  MeV. Using Eq. (6b) then yields the estimate  $\epsilon_m(\text{type II}) = 16.6$  MeV. Likewise, guessing  $J_{\text{av}} = 30$  gives  $\epsilon_m(\text{type III}) = 10.8$  MeV. These are the estimates used in a companion paper,<sup>13</sup> where the data for the Au<sup>197</sup>+C<sup>12</sup> system are reproduced. We see that the experimental results are not inconsistent with the contribution of a sizeable subspectrum peak near 16 MeV, although the data cannot be unequivocally interpreted in this energy range.

<sup>34</sup> A. G. W. Cameron and R. M. Elkin, Goddard Institute for Space Studies Report, 1965 (unpublished).

<sup>35</sup> J. H. E. Mattauch, W. Thiele, and A. H. Wapstra, Nucl. Phys. **67**, 32 (1965).

<sup>36</sup> T. D. Thomas, Phys. Rev. **116**, 703 (1959).